

Magnetic resonance studies of Co^{2+} ions in nanoparticles of SnO_2 processed at different temperatures

Sushil K. Misra^{a)} and Serguei I. Andronenko

Department of Physics, Concordia University, 1455 de Maisonneuve Boulevard West, Montreal, Quebec H3G 1M8, Canada

K. M. Reddy, J. Hays, and A. Punnoose

Department of Physics, Boise State University, Boise, Idaho 83725-1570

(Presented on 2 November 2005; published online 19 April 2006)

Cobalt doping ($\leq 1\%$) produces ferromagnetism at room temperature in semiconducting SnO_2 , presumably due to oxygen vacancies and/or changes in carrier concentration. Electron paramagnetic resonance (EPR) is a sensitive technique to investigate the Co ionic states and their local environments and/or interactions. This paper reports EPR studies of Co^{2+} ions doped in chemically synthesized nanoparticles of SnO_2 carried out at 5 K. EPR spectra were recorded from 600 °C prepared SnO_2 with Co concentrations of 0.5%, 1%, 3%, 5%, 8%, and 12% and from 1% Co-doped SnO_2 prepared at temperatures of 150, 250, 350, 450, 600, and 830 °C. Each EPR spectrum in samples with cobalt doping can be simulated as an overlap of spectra due to two broad ferromagnetic resonance lines and those due to interstitially and substitutionally incorporated Co^{2+} ions with effective spin $S=1/2$ characterized by their particular \mathbf{g} and \mathbf{A} tensors. It is concluded that the Co^{2+} ions occupy substitutional as well as interstitial sites of SnO_2 and that a fraction, albeit small, of the doped Co^{2+} spins contribute to the ordered ferromagnetic state. The relative concentrations of these different components depend on the annealing temperature and Co concentration of the samples. © 2006 American Institute of Physics. [DOI: 10.1063/1.2165146]

Tin dioxide (SnO_2), a chemically stable transparent oxide semiconductor with a band gap of ~ 3.6 eV, is an attractive system for a wide variety of practical applications.¹⁻⁶ It has been shown⁷⁻¹⁰ that Co doping produces ferromagnetism in SnO_2 , thus making it a promising ferromagnetic semiconductor at room temperature. This is a very important step in producing practically useful spintronic devices, which use the spin of the particles in addition to their charges. Several devices such as spin transistors, spin light-emitting diodes (LEDs), very high-density nonvolatile semiconductor memory, and optical emitters with polarized output have been proposed using these materials.¹¹⁻¹⁴ The presence of oxygen vacancies is crucial in producing the ferromagnetism in transition-metal-doped semiconductor oxides.^{15,16}

Detailed synthesis procedures of the samples investigated in this work have been reported elsewhere.^{7,9} Based on quantitative magnetic measurements, it was shown that chemically synthesized $\text{Sn}_{1-x}\text{Co}_x\text{O}_2$ powders exhibit room-temperature ferromagnetism for $x \leq 0.01$ when prepared in the 350–600 °C range. Magnetic hysteresis loops observed in $\text{Sn}_{0.99}\text{Co}_{0.01}\text{O}_2$ powder at 300 K displayed large coercivity $H_c \sim 630$ Oe, saturation magnetization $M_s \sim 0.133 \mu_B/\text{Co}$ ion and about 31% remanence, and with a Curie temperature $T_c = 450$ K.⁸ However, for $x > 0.01$, no such ferromagnetism was observed at room temperature, and the samples demonstrated a paramagnetic behavior. Here we report the detailed electron paramagnetic resonance (EPR) investigations of these samples with a specific interest to understand how the Co ions are incorporated into the SnO_2 lattice and how they interact with their environment.

Figures 1 and 2 show EPR spectra at 5 K as recorded on a Bruker X-band spectrometer, equipped with an Oxford Instruments variable-temperature accessory for 600 °C prepared samples with different amounts of Co doping (0.5%, 1%, 3%, 5%, 8%, and 12%) and for samples with 1% Co doping prepared at different temperatures (150, 250, 350, 450, 600, and 830 °C). The EPR signals are poor at room and higher temperatures for the cobalt ion due to very short spin-lattice relaxation times which broaden the lines considerably, making it difficult to study the temperature variation of cobalt spectrum. A visual inspection of the various spectra reveals that there exists an overlap of two broad ferromagnetic resonance (FMR) lines and those due to interstitially and substitutionally incorporated Co^{2+} ions with effective spin $S=1/2$. The fact that the Co EPR spectra are due to low-spin ($S=1/2$) and not due to high-spin species ($S=3/2$) is revealed by the absence of the three allowed fine-structure lines expected for the high-spin Co. This is in accordance with the fact that at liquid-helium temperatures the ions are predominantly in the lowest-lying Kramers doublet. In the paramagnetic state the spin Hamiltonian characterizing the spin-1/2 state is $\mathcal{H}_S = \mathbf{g}\mu_B\mathbf{B}\cdot\mathbf{g}\cdot\mathbf{S} + \mathbf{S}\cdot\mathbf{A}\cdot\mathbf{I}$, where \mathbf{g} , \mathbf{A} , μ_B , \mathbf{B} , \mathbf{S} , and \mathbf{I} are the \mathbf{g} tensor, hyperfine-interaction tensor, the Bohr magneton, external magnetic field, electron spin, and nuclear spin, respectively. The spectra simulated here were done using the Bruker Simfonia software assuming possible contributions due to (i) isolated Co^{2+} ions substitutionally incorporated into the SnO_2 lattice, (ii) isolated interstitial Co^{2+} ions, and (iii) two main backgrounds due to ferromagnetically coupled Co^{2+} spins. Evidence for the presence of all these three contributions has been recently reported by Hays *et al.*⁹ based on detailed studies using mag-

^{a)}Electronic mail: skmisra@vax2.concordia.ca

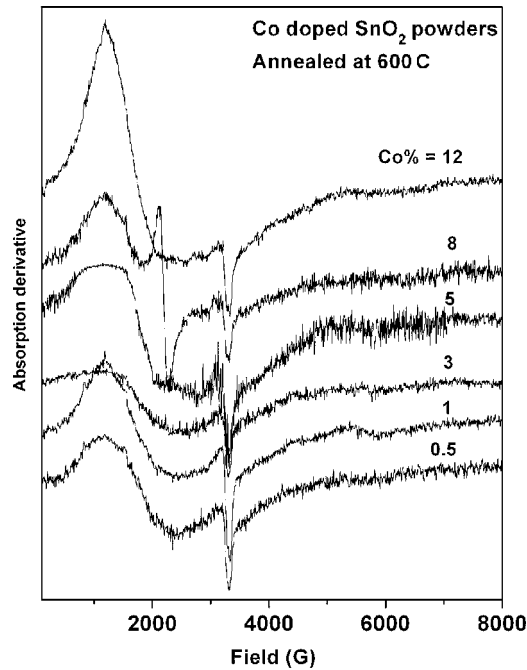


FIG. 1. X-band EPR spectra for Co doped samples with different Co-dopings, recorded at 5 K. The additional peak observed only in the 8% Co-doped sample is ignored in the analysis assuming it to be due to an unknown impurity.

netometry, x-ray diffraction, Raman spectroscopy, and x-ray photoelectron spectroscopy. The simulated individual spectra for these possible contributions are shown as insets (a), (b), (c), and (d) in Fig. 3. Insets (a) and (b) show the simulated spectra for two first-derivative FMR resonances (FMR1 and FMR2) with a Gaussian line shape (considering inhomogeneous broadening inherent in amorphous/nanoscale samples), characterized by different peak positions and line-

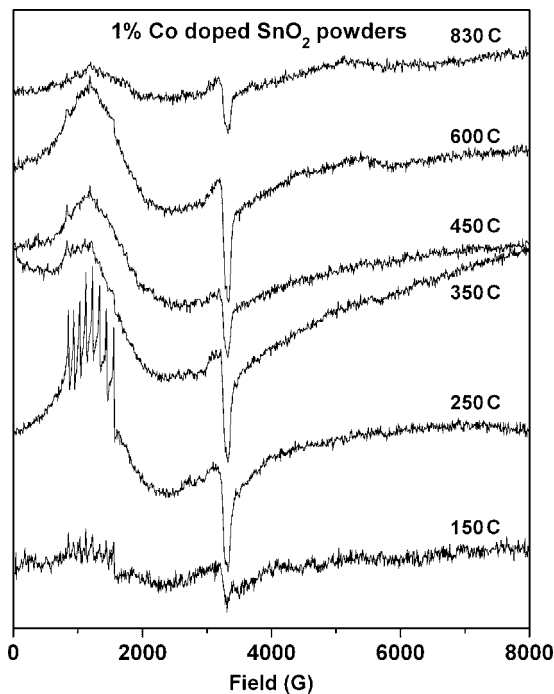


FIG. 2. X-band EPR spectra of 1.0% Co-doped samples fabricated at different temperatures recorded at 5 K.

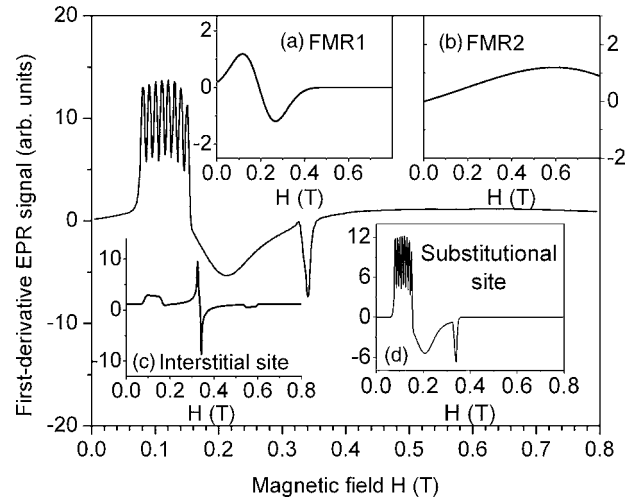


FIG. 3. The insets show simulated spectra for (a) simulated first-derivative FMR resonances (FMR1), (b) simulated first-derivative broad resonances (FMR2) (c) that due to a Co^{2+} ion in an interstitial position, and (d) that due to a Co^{2+} ion in a substitutional site. The main figure shows a weighted overlap of the four individual components shown in insets (a) through (d) to correspond to the experimental spectrum for the sample fabricated at 250 °C as shown in Fig. 2. The other observed spectra can be simulated by appropriate weightings of the four constituent spectra and linewidths.

widths. The simulated spectra for a Co^{2+} ion in an interstitial position with effective spin $S=1/2$ is shown in inset (c) and that due to a Co^{2+} ion in a substitutional site with effective spin $S=1/2$ is shown in inset (d). The g - and A -tensor values and the linewidth ΔB of these components employed in the simulation are given in Table I. The overlapped spectrum is shown in Fig. 3 combining these four contributions with appropriate weights to resemble that observed experimentally for the 1.0% Co-doped SnO_2 annealed at 250 K (shown in Fig. 2). All other spectra in Figs. 1 and 2 can easily be simulated by including appropriate contributions of component signals shown in insets (a) through (c) in Fig. 3 and by varying the linewidths. Increasing the linewidth suppresses hyperfine splitting which is clearly observed in samples annealed at ≤ 250 °C.

It was observed in our recent studies⁷⁻⁹ that the predominant phase formed in Co-doped tin oxide samples prepared by annealing the reaction precipitate at temperatures below 350 °C is tin monoxide (SnO), which gets converted to tin dioxide (SnO_2) when annealed at higher temperatures (≥ 350 °C). It is well known that the p -type semiconducting behavior of SnO results from an excess of oxygen, whereas the existence of oxygen vacancies in SnO_2 make it an excellent n -type semiconductor.^{8,16} Moreover, x-ray photoelectron spectroscopy measurements showed that the oxygen content decreases with increasing Co doping in SnO_2 .⁹ Based on these results, the absence of the hyperfine splitting in samples prepared at temperatures ≥ 350 °C can be attributed to an increasing number of randomly distributed defects, which enhances disorder of the crystalline field at Co^{2+} sites, thereby increasing the hyperfine linewidth. With increasing Co concentration, the spin-spin interactions also contribute to the broadening of the lines. In our magnetic studies,^{7,9} a high-spin Co^{2+} state with $S=3/2$ was indicated. However, as mentioned above, the EPR spectral parameters indicated an

TABLE I. The g - and A -tensor values and the linewidths ΔB of the interstitial and substitutional Co ions employed in the simulation of the EPR spectra.

EPR active species	g_x	g_y	g_z	A_x (mT)	A_y (mT)	A_z (mT)	ΔB_x (mT)	ΔB_y (mT)	ΔB_z (mT)	
Substitutional Co^{2+}	2.05	4.0	6.0	1.0	10.0	10.0	5.0	30.0	4.0	
Interstitial Co^{2+}	1.20	2.05	5.80	7.0	1.0	10.0	10.0	5.0	15.0	
FMR1	3.4 (isotropic)						170 (isotropic)			
FMR2	0.6 (isotropic)						1100 (isotropic)			

effective spin of $S=1/2$, which is due to the fact that at the low temperature (5 K) employed for EPR measurements, only the lowest doublet of the high-spin Co^{2+} is populated.

The EPR spectral parameters of the substitutional Co^{2+} ions are close to those reported for Co^{2+} incorporated in similar sites in other host systems.^{17,18} Accordingly, here the crystal symmetry is tetrahedral, the same as that of the isostructural crystal rutile TiO_2 ,^{17,18} which results in the site symmetry of the substitutional site being octahedral due to the surrounding oxygen tetrahedron. The same is expected of the interstitial site. This accounts appropriately for the low-spin state of cobalt observed here, and the corresponding hyperfine coupling. The nature and spectral parameters of the FMR1 signal are similar to those reported for magnetic nanoparticle systems below their blocking temperatures.^{19,20} Both the shift of the observed signal to lower fields and the linewidth are related to the anisotropy in nonspherical particles with a statistical distribution of sizes and shapes.¹⁹ Transmission electron microscopy measurements⁷ have shown the presence of nonspherical nanoscale particles in these samples. Using magnetometry measurements, clear evidence for room-temperature ferromagnetism was observed in samples with $\leq 1\%$ Co and the relatively higher intensity of the FMR1 component in these samples support these results.⁹ However, analysis of the EPR data shown in Fig. 1 indicates the presence of an FMR1 component in the samples with Co concentration $>1\%$ also, albeit much weaker in strength. This may be due to the presence of a small fraction of ferromagnetically ordered particles in the samples with $>1\%$ Co also, but presumably with blocking temperatures <300 K. Interestingly, the average particle size of the samples is found to decrease with increasing Co concentration, with ~ 60 nm for undoped SnO_2 particles to ~ 20 nm for 8% Co-doped SnO_2 ,⁹ suggesting that Co incorporation reduces the nucleation and growth of the SnO_2 particles. Blocking temperatures of magnetic nanoparticles have been reported to decrease with decreasing particle size. The origin of the FMR2 component is, however, not fully understood at present. This primarily accounts for the broad background signal present in most samples. The Co ions distributed in random locations might be one possible source of this overall EPR background.

The simulations presented here help understand the main EPR spectral features. In finer detail, each observed spectrum consists of the overlap of spectra due to additional Co ions in interstitial and substitutional sites. The peak height of the FMR1 component line and that of the signal at $g \sim 2$ are indicative of the ferromagnetism and the presence of Co ions in the paramagnetic state in a qualitative manner. The presence of both paramagnetic spins and ferromagnetically or-

dered components have been reported to be present in transition-metal-doped semiconductor oxide systems.^{11,12} A detailed microscopic analysis of the observed spectra will require an exorbitant effort which is not warranted over and above the main properties of the magnetic properties already deduced.

The EPR measurements presented in this paper reveal that Co doping results in both a ferromagnetically ordered component and isolated paramagnetic Co^{2+} ions incorporated into the SnO_2 lattice. Evidence for both substitutional and interstitial incorporation of Co were observed in the EPR spectra. In samples with Co doping greater than 1%, the spectra were constituted by signals due to Co^{2+} ions in interstitial and substitutional sites over a presumably non-FMR background.

We acknowledge financial support from the NSF-Idaho-EPSCoR Program, the NSF awards EPS-0447689 and DMR-0321051, and CAREER award DMR-0449639 (KMR, JH, AP), and the NSERC Canada (SKM).

- ¹E. J. H. Lee, C. Ribeiro, T. R. Giraldo, E. Longo, E. R. Leite, and J. A. Varela, *Appl. Phys. Lett.* **84**, 1745 (2004).
- ²N. Chiodini, A. Paleari, D. DiMartino, and G. Spinolo, *Appl. Phys. Lett.* **81**, 1702 (2002).
- ³P. G. Harrison, N. C. Lloyd, and W. Daniell, *J. Phys. Chem. B* **102**, 10672 (1998).
- ⁴S.-C. Lee, J.-H. Lee, T.-S. Oh, and Y.-H. Kim, *Sol. Energy Mater. Sol. Cells* **75**, 481, 2003.
- ⁵S. A. Pianaro, P. R. Bueno, E. Longo, and J. A. Varela, *J. Mater. Sci. Lett.* **14**, 692 (1995).
- ⁶E. A. Bondar, S. A. Gormin, I. V. Petrochenko, and L. P. Shadrina, *Opt. Spectrosc.* **89**, 892 (2000).
- ⁷A. Punnoose, J. Hays, V. Gopal, and V. Shutthanandan, *Appl. Phys. Lett.* **85**, 1559 (2004).
- ⁸A. Punnoose and J. Hays, *J. Appl. Phys.* **97**, 10D321 (2005).
- ⁹J. Hays, A. Punnoose, R. Baldner, M. H. Engelhard, J. Peloquin, and K. M. Reddy, *Phys. Rev. B* (in press).
- ¹⁰S. B. Ogale *et al.*, *Phys. Rev. Lett.* **91**, 077205 (2003).
- ¹¹G. A. Prinz, *Science* **282**, 1660 (1998); *J. Magn. Magn. Mater.* **200**, 57 (1999).
- ¹²S. A. Chambers and R. F. C. Farrow, *MRS Bull.* **28**, 729 (2003).
- ¹³S. J. Pearton *et al.*, *J. Appl. Phys.* **93**, 1 (2003).
- ¹⁴N. Lebedeva and P. Kuivalainen, *J. Appl. Phys.* **93**, 9845 (2003).
- ¹⁵J. M. D. Coey, A. P. Douvalis, C. B. Fitzgerald, and M. Venkatesan, *Appl. Phys. Lett.* **84**, 1332 (2004).
- ¹⁶A. Punnoose, J. Hays, A. Thurber, M. H. Engelhard, R. K. Kukkadapu, C. Wang, V. Shutthanandan, and S. Thevuthasan, *Phys. Rev. B* **72**, 054402 (2005).
- ¹⁷E. Yamaka and R. G. Barnes, *Phys. Rev.* **125**, 1568 (1962).
- ¹⁸Y. Miyako and Y. Kazumata, *J. Phys. Soc. Jpn.* **31**, 1727 (1971); Y. Miyako, *Phys. Lett.* **24A**, 635 (1967).
- ¹⁹K. Nagata and A. Ishihara, *J. Magn. Magn. Mater.* **104–107**, 1571 (1992).
- ²⁰A. Punnoose, M. S. Seehra, J. van Tol, and L. C. Brunel, *J. Magn. Magn. Mater.* **288**, 168 (2005); A. Punnoose and M. S. Seehra, in *EPR in the 21st Century*, edited by A. Kawamori, J. Yamauchi, and H. Ohta (Elsevier, New York, 2002) p. 162.